VERY FAST ALGORITHMS AND DETECTION PERFORMANCE OF MULTI-CHANNEL AND 2-D PARAMETRIC ADAPTIVE MATCHED FILTERS FOR AIRBORNE RADAR

S. Lawrence Marple Jr.[*]

School of Electrical Engineering
and Computer Science
Oregon State University
Corvallis, OR 97331
marple@eecs.oregonstate.edu

Phillip M. Corbell, Muralidhar Rangaswamy[†]

Air Force Research Laboratory
Sensors Directorate
Hanscom AFB, MA 01731
phillip.corbell@hanscom.af.mil,
muralidhar.rangaswamy@hanscom.af.mil

ABSTRACT

In a seminal paper [1] published in 2000, two algorithmic versions of the multichannel parametric adaptive matched filter (PAMF) applied to space-time adaptive processing (STAP) in an airborne radar application were shown to achieve superior test detection statistics over the conventional adaptive matched filter (AMF), which uses a non-parametric approach to estimate the detection weight vector. In fact, the performance of the PAMF approach is very close to the ideal matched filter (MF) detection statistics under exactly known covariance (the clairvoyant case). Improved versions of the two original multichannel PAMF algorithms [5], one new multichannel PAMF algorithm [6], and a new two-dimensional (2D) PAMF algorithm [all four with fast computational implementations] have been recently developed. In this paper, we provide the outline of the new 2D parametric algorithm and summarize the detection performance of 3 of the 4 new PAMF algorithms with actual Multi-Channel Airborne Radar Measurement (MCARM) data. In all cases, the performance is at least comparable to, and in some cases superior to, the original multichannel PAMF algorithms presented in [1], while also achieving computational savings over the originals.

1. INTRODUCTION

In STAP [2], the output $y = \mathbf{w}^T\mathbf{x}$ of a linear combiner (space-time filter) operating on the radar system sensor array is expressed in terms of an inner product of a multi-channel (MC) weight vector $\mathbf{w}$ of dimension $M \times 1$ and a comparable dimension MC data vector from the array. It is well known that the optimal (adaptive) weights that minimize the variance of the output y while passing a signal from a preferred steering vector direction, represented by the vector $\mathbf{e}$, is

$$\mathbf{w} = \mathbf{R}^{-1}\mathbf{e} \tag{1}$$

[*]Dr. Marple's research supported by the Air Force Office of Scientific Research (AFOSR) under the Summer Faculty Fellowship Program (SFFP) administered by the American Society for Engineering Education (ASEE)

[†]Dr. Rangaswamy's research supported by AFOSR under project 2304

in which the MC covariance matrix $\mathbf{R}_d$ is based on the second-order statistics of the disturbance (no target), which consists of terrain clutter noise plus interferences plus receiver white noise. A matched filter (MF) detection statistic [1] is evaluated by comparing the value of

$$\Lambda_{\mathrm{MF}} = \frac{\left|\mathbf{e}^H\mathbf{R}_d^{-1}\mathbf{x}\right|^2}{\mathbf{e}^H\mathbf{R}_d^{-1}\mathbf{e}}, \tag{2}$$

in which $\mathbf{e}$ is steering vector and $\mathbf{x}$ is the current measurement vector, to a threshold that sets the probability of false alarm. In practice, the adaptive matched filter (AMF) detection statistic

$$\Lambda_{\mathrm{AMF}} = \frac{\left|\mathbf{e}^H\hat{\mathbf{R}}_d^{-1}\mathbf{x}\right|^2}{\mathbf{e}^H\hat{\mathbf{R}}_d^{-1}\mathbf{e}} \tag{3}$$

is evaluated by taking the inverse of the estimated covariance matrix

$$\hat{\mathbf{R}}_d = \frac{1}{R}\sum_{r=1}^{R}\mathbf{x}[r]\mathbf{x}^H[r] \tag{4}$$

over R measured realizations of the MC data vector $\mathbf{x}$ of dimension M. This is usually very computationally intensive if the dimension of the M-channel system, which is typically the product of the number of array channels with the number of pulses processed, is in the hundreds. As an alternative to the AMF, [1] and [5] discovered that multi-channel and two-dimensional parametric estimation approaches could (1) reduce the computational requirements by reducing the covariance matrix dimension while (2) improving the detection performance over the traditional AMF approach. Both enhancements were achieved by replacing the inverse of the estimated covariance matrix of the disturbance with the order $p << M$ parametric alternative

$$\boxed{\hat{\underline{\mathbf{R}}}_d^{-1} = \underline{\mathbf{A}}_p^H\underline{\mathbf{P}}_p^a\underline{\mathbf{A}}_p - \underline{\mathbf{B}}_p^H\underline{\mathbf{P}}_p^b\underline{\mathbf{B}}_p} \tag{5}$$

in which the block triangular Toeplitz matrix structures, developed in [6], are functions of the forward MC linear predic-

Report Documentation Page

Form Approved
OMB No. 0704-0188

1. REPORT DATE	2. REPORT TYPE	3. DATES COVERED
01 APR 2008	**N/A**	**-**

4. TITLE AND SUBTITLE	5a. CONTRACT NUMBER
Very Fast Algorithms and Detection Performance Of Multi-Channel and 2-D Parametric Adaptive Matched Filters for Airborne Radar Applications	5b. GRANT NUMBER
	5c. PROGRAM ELEMENT NUMBER
6. AUTHOR(S)	5d. PROJECT NUMBER
	5e. TASK NUMBER
	5f. WORK UNIT NUMBER
7. PERFORMING ORGANIZATION NAME(S) AND ADDRESS(ES) **School of Electrical Engineering and Computer Science Oregon State University Corvallis, OR 97331**	8. PERFORMING ORGANIZATION REPORT NUMBER
9. SPONSORING/MONITORING AGENCY NAME(S) AND ADDRESS(ES)	10. SPONSOR/MONITOR'S ACRONYM(S)
	11. SPONSOR/MONITOR'S REPORT NUMBER(S)

12. DISTRIBUTION/AVAILABILITY STATEMENT
Approved for public release, distribution unlimited

13. SUPPLEMENTARY NOTES
See also ADM002078., The original document contains color images.

14. ABSTRACT

15. SUBJECT TERMS

16. SECURITY CLASSIFICATION OF:			17. LIMITATION OF ABSTRACT	18. NUMBER OF PAGES	19a. NAME OF RESPONSIBLE PERSON
a. REPORT	b. ABSTRACT	c. THIS PAGE			
unclassified	**unclassified**	**unclassified**	**UU**	**35**	

tion error of model order p and realization r

$$\mathbf{e}_p^a[n;r] = \mathbf{x}[n;r] + \sum_{k=1}^{p} \mathbf{A}_p[k]\mathbf{x}[n-k;r], \quad (6)$$

the backward MC linear prediction error of similar model order p

$$\mathbf{e}_p^b[n;r] = \mathbf{x}[n-p;r] + \sum_{k=1}^{p} \mathbf{B}_p[k]\mathbf{x}[n-p+k;r], \quad (7)$$

and the forward and backward linear prediction error variances, which are respectively

$$\mathbf{P}_p^a = \mathcal{E}\left\{\mathbf{e}_p^a[n](\mathbf{e}_p^a[n])^H\right\}, \mathbf{P}_p^b = \mathcal{E}\left\{\mathbf{e}_p^b[n](\mathbf{e}_p^b[n])^H\right\}. \quad (8)$$

The MC parameter matrices $\mathbf{A}_p[k]$, $\mathbf{B}_p[k]$, $\mathbf{P}_p^a$, and $\mathbf{P}_p^b$ are estimated by fast computational algorithms, as discussed in [3] and [6]. One algorithm is based on the MC harmonic-mean least-squares-based lattice algorithm developed by Nuttall-Strand [3] [reference as MC-LLS] and the other is based on the MC geometric-mean non-least-squares lattice algorithm developed by Viera-Morf [3] [reference as MC-LGM]. The resulting parametric adaptive matched filter [PAMF] detection statistic for these two algorithms takes the form

$$\Lambda_{\mathrm{PAMF-MF}} = \frac{\left|\sum_{n=1}^{N-p} \mathbf{e}[n]^H \mathbf{R}_d^{-1} \mathbf{x}[n]\right|^2}{\sum_{n=1}^{N-p} \mathbf{e}[n]^H \mathbf{R}_d^{-1} \mathbf{e}[n]} \quad (9)$$

which uses the parametric inversion formula Eq. 5, and N is the number of pulses processed. An exact least-squares-based MC covariance case of MC linear prediction uses yet another form for the inverse matrix, specifically

$$\boxed{\begin{aligned}\left(\underline{\mathbf{X}}_p \underline{\mathbf{X}}_p^H\right)^{-1} &= \underline{\mathbf{A}}_p \underline{\mathbf{P}}_p^a \underline{\mathbf{A}}_p^H - \underline{\mathbf{B}}_p \underline{\mathbf{P}}_p^b \underline{\mathbf{B}}_p^H \\ &+ \underline{\mathbf{C}}_{p-1} \underline{\mathbf{P}}_p^c \underline{\mathbf{C}}_{p-1}^H - \underline{\mathbf{D}}_{p-1} \underline{\mathbf{P}}_p^d \underline{\mathbf{D}}_{p-1}^H\end{aligned}} \quad (10)$$

in which the various block triangular Toeplitz matrix terms come out of the fast computational algorithm discussed in [3]. The inverse Eq. 10 is used in lieu of $\hat{\mathbf{R}}_d$ in the PAMF statistic. A fourth scheme, covered in this paper, is based on two-dimensional (2-D) parametric estimation using the 2-D least-squares-based lattice algorithm [4]. The specifics of the inverse are found in the next section of this paper. The resulting 2D PAMF detection statistic will take the form

$$\Lambda_{\mathrm{PAMF-2D}} = \frac{\left|\sum_{j=1}^{J-q}\sum_{n=1}^{N-p} \mathbf{e}[j,n]^H \hat{\mathbf{R}}_d^{-1} \mathbf{x}[j,n]\right|^2}{\left[\sum_{j=1}^{J-q}\sum_{n=1}^{N-p} \mathbf{e}[j,n]^H \hat{\mathbf{R}}_d^{-1} \mathbf{e}[j,n]\right]} \quad (11)$$

in which two parametric orders p [the pulse dimension] and q [the array element dimension] will be required.

2. 2D LEAST-SQUARES LINEAR PREDICTION PARAMETER ESTIMATION

The 2-D forward linear prediction error (LPE) of model order $p2$ for the 2-D signal $x[n1, n2; r]$ and dimension $(p1+1) \times (N1-p1)$ is defined as

$$\mathbf{e}_{p2}^a[n;r] = \mathbf{X}[n;r] + \sum_{k=1}^{p2} \mathbf{A}_{p2}[k]\mathbf{X}[n-k;r] \quad (12)$$

over $p2+1 \le n2 \le N2$, in which $\mathbf{A}_{p2}[k]$ are the 2-D forward linear prediction parameters of dimension $(p1+1)\times(p1+1)$. This may be expressed in vector inner product form as

$$\mathbf{e}_{p2}^a[n;r] = \begin{pmatrix}\mathbf{I} & \underline{\mathbf{A}}_{p2}\end{pmatrix} \underline{\mathbf{X}}_{p2}[n;r] \quad (13)$$

for which $\underline{\mathbf{A}}_{p2} = (\mathbf{A}_{p2}[1] \ldots \mathbf{A}_{p2}[p2])$ is a $1 \times p2$ block row vector [scalar dimension $(p1+1) \times (p1+1)p2$] of the 2-D forward LP parameters and $\mathbf{X}[n;r] =$

$$\begin{pmatrix} x[p1,k;r] & \cdots & x[N1-1,k;r] \\ \vdots & \ddots & \vdots \\ x[N1-p1-1,k;r] & & x[p1,k;r] \\ \vdots & \ddots & \vdots \\ x[0,k;r] & \cdots & x[N1-p1-1,k;r] \end{pmatrix} \quad (14)$$

is a $(p1+1) \times (N1-p1)$ data matrix and

$$\underline{\mathbf{X}}_{p2}[n;r] = \begin{pmatrix} \mathbf{X}[n;r] \\ \vdots \\ \mathbf{X}[n-p2;r] \end{pmatrix} \quad (15)$$

is a $(p1+1)(p2+1) \times (N1-p1)$ block column vector of data matrices. Similarly, the 2-D backward linear prediction error (LPE) is defined as

$$\begin{aligned}\mathbf{e}_{p2}^b[n;r] &= \mathbf{X}[n-p2;r] + \sum_{k=1}^{p2} \mathbf{B}_{p2}[k]\mathbf{X}[n-p2+k;r] \\ &= \begin{pmatrix}\underline{\mathbf{B}}_{p2} & \mathbf{I}\end{pmatrix} \underline{\mathbf{X}}_{p2}[n;r]\end{aligned}$$

for which $\underline{\mathbf{B}}_{p2} = (\mathbf{B}_{p2}[p2] \ldots \mathbf{B}_{p2}[1])$ is a $1 \times p2$ block row vector [scalar dimension $(p1+1) \times (p1+1)p2$] of the 2-D backward LP parameters (note that the backward LP parameter vector has reversed indexing relative to the forward LP parameter vector). The $(p1+1) \times (p1+1)$ 2-D forward LPE variance is both defined and expressed as

$$\mathbf{P}_{p2}^a = \mathcal{E}\left\{\mathbf{e}_{p2}^a(\mathbf{e}_{p2}^a)^H\right\} = \begin{pmatrix}\mathbf{I} & \underline{\mathbf{A}}_{p2}\end{pmatrix} \underline{\mathbf{R}}_{p2} \begin{pmatrix}\mathbf{I} \\ \underline{\mathbf{A}}_{p2}^H\end{pmatrix} \quad (16)$$

in which $\underline{\mathbf{R}}_{p2}$ is the block $(p2+1) \times (p2+1)$ 2-D double Toeplitz autocovariance matrix [it is also hermitian symmetric] with a scalar dimension of $(p1+1)(p2+1) \times (p1+$

$1)(p2+1)$ with structure

$$\begin{pmatrix} \mathbf{R}[0] & \cdots & \mathbf{R}[p2-1] & \mathbf{R}[p2] \\ \mathbf{R}[-1] & \cdots & \mathbf{R}[p2-2] & \mathbf{R}[p2-1] \\ \vdots & \ddots & \vdots & \vdots \\ \mathbf{R}[-(p2-1)] & \cdots & \mathbf{R}[0] & \mathbf{R}[1] \\ \mathbf{R}[-p2] & \cdots & \mathbf{R}^*[1] & \mathbf{R}[0] \end{pmatrix} \quad (17)$$

composed of the stationary $(p1+1)\times(p1+1)$ scalar-dimensioned 2-D autocovariance matrix elements $\mathbf{R}[k] =$

$$\begin{pmatrix} r[0,k] & r[1,k] & \cdots & r[p1,k] \\ r[-1,k] & r[0,k] & \cdots & r[p1-1,k] \\ \vdots & \vdots & \ddots & \vdots \\ r[-p1,k] & r[-(p1-1),k] & \cdots & r[0,k] \end{pmatrix}. \quad (18)$$

Note that $\underline{\mathbf{R}}_{p2}$ is double Toeplitz (Toeplitz at the block level and also the block matrix elements themselves are Toeplitz); this property results in the relationship $\underline{\mathbf{R}}_{p2} = \mathbf{J}\underline{\mathbf{R}}^*_{p2}\mathbf{J}$ and $\underline{\mathbf{R}}_{p2} = \underline{\mathbf{R}}^H_{p2}$. In a similar manner, the 2-D $(p1+1)\times(p1+1)$ backward LPE variance is given by

$$\underline{\mathbf{P}}^b_{p2} = \mathcal{E}\left\{\mathbf{e}^b_{p2}(\mathbf{e}^b_{p2})^H\right\} = \left(\underline{\mathbf{B}}_{p2} \;\; \mathbf{I}\right)\underline{\mathbf{R}}_{p2}\begin{pmatrix} \underline{\mathbf{B}}^H_{p2} \\ \mathbf{I} \end{pmatrix}. \quad (19)$$

Assuming the initialization $\mathbf{P}_0 = \mathbf{R}[0]$, the four steps of the 2-D Levinson recursion, that solves for the LP parameters $\underline{\mathbf{A}}_k$ and 2-D LPE variance $\mathbf{P}_k$ over $k = 1, \ldots, p$, are

$$\mathbf{\Delta}_k = \left(\mathbf{I} \;\; \underline{\mathbf{A}}_{k-1}\right)\begin{pmatrix} \mathbf{R}[k] \\ \vdots \\ \mathbf{R}[1] \end{pmatrix} = \mathbf{J}\mathbf{\Delta}^T_k\mathbf{J} \quad (20)$$

$$\mathbf{\Gamma}_k = -\mathbf{\Delta}_k\left(\mathbf{J}\mathbf{P}^*_{k-1}\mathbf{J}\right)^{-1} \quad (21)$$

$$\left(\mathbf{I} \;\; \underline{\mathbf{A}}_k\right) = \left(\mathbf{I} \;\; \underline{\mathbf{A}}_{k-1} \;\; \mathbf{0}\right) + \mathbf{\Gamma}_k\left(\mathbf{0} \;\; \mathbf{J}\underline{\mathbf{A}}^*_{k-1}\mathbf{J} \;\; \mathbf{I}\right) \quad (22)$$

$$\mathbf{P}_k = \left(\mathbf{I} - \mathbf{\Gamma}_k\left(\mathbf{J}\mathbf{\Gamma}^*_k\mathbf{J}\right)\right)\mathbf{P}_{k-1}. \quad (23)$$

This will reduce to 1-D Levinson recursion when $p1 = 0$;

3. PARAMETRIC INVERSE OF 2D DOUBLY TOEPLITZ COVARIANCE MATRIX

The form of the doubly Toeplitz block inverse [4] which is useful to this project, and which also depends only on the last parameter order computed, is

$$\boxed{\underline{\mathbf{R}}^{-1}_{p2} = \underline{\mathbf{A}}^H_{p2}\underline{\mathbf{P}}^A_{p2}\underline{\mathbf{A}}_{p2} - \underline{\mathbf{B}}^H_{p2}\underline{\mathbf{P}}^B_{p2}\underline{\mathbf{B}}_{p2}} \quad (24)$$

in which the block triangular Toeplitz matrices are given as

$$\underline{\mathbf{A}}_{p2} = \begin{pmatrix} \mathbf{I} & \mathbf{A}_{p2}[1] & \cdots & \mathbf{A}_{p2}[p2] \\ \mathbf{0} & \ddots & \ddots & \vdots \\ \vdots & \ddots & \ddots & \mathbf{A}_{p2}[1] \\ \mathbf{0} & \cdots & \mathbf{0} & \mathbf{I} \end{pmatrix} \quad (25)$$

$$\underline{\mathbf{B}}_{p2} = \begin{pmatrix} \mathbf{0} & \mathbf{B}_{p2}[p2] & \cdots & \mathbf{B}_{p2}[1] \\ \mathbf{0} & \ddots & \ddots & \vdots \\ \vdots & \ddots & \ddots & \mathbf{B}_{p2}[p2] \\ \mathbf{0} & \cdots & \mathbf{0} & \mathbf{0} \end{pmatrix} \quad (26)$$

$$\underline{\mathbf{P}}^A_{p2} = \begin{pmatrix} (\mathbf{P}_{p2})^{-1} & \mathbf{0} & \cdots & \mathbf{0} \\ \mathbf{0} & \ddots & \ddots & \vdots \\ \vdots & \ddots & \ddots & \mathbf{0} \\ \mathbf{0} & \cdots & \mathbf{0} & (\mathbf{P}_{p2})^{-1} \end{pmatrix}. \quad (27)$$

The block diagonal matrix $\underline{\mathbf{P}}^B_{p2}$ is similar to $\underline{\mathbf{P}}^A_{p2}$, except the block diagonal elements are $(\mathbf{J}\mathbf{P}^*_{p2}\mathbf{J})^{-1}$.

4. PERFORMANCE ANALYSIS USING ACTUAL MCARM RADAR DATA

For details on the motivation and structure of the MCARM radar data, the reader is referred to Section C of reference [1]. A key issue in performance testing, specifically the probability of detection P_{D}, is the amount of secondary (training) data [small vs large sample sizes] required to achieve a reasonable level of detection performance in a constant false alarm rate P_{FA} (CFAR) scenario. Three scenarios that inject artificial target signals into the actual MCARM data were considered, leading to eight plot sets of test statistic magnitude vs range bin index for various multi-channel and 2D algorithm order selections. The MCARM database used for this analysis extracted (from acquisition 575, flight 5) one elevation channel, 4 azimuth channels, 32 pulses, and inclusive range bins (RBs) 142-469 from each pulse. In test case 1, a fixed window of training data utilized 256 RBs (142-269 and 341-468), a pair of simulated primary targets with an input SINR of -30 dB were inserted into RBs 291 and 293, and the appropriate detection test statistic (either MC Eq. 9 or 2D Eq. 11) generated from RBs 270-340 for plotting. In test case 2, a moving window of training data consisted of 11 adjacent RBs centered sequentially over RBs 270-340, with the same simulated primary targets inserted into RBs 291 and 293, and the test statistics then generated. The three center RBs in the moving window were not used in the estimate of the inverse covariance, leaving only a short 8 RB secondary data sequence (in contrast to the long 256 RB test case 1). The test case 3 is identical to test case 1, except four secondary disturbance targets were artifically inserted into RBs 238, 269, 373, and 400, each with an input SINR of -10 dB and the same steering vectors as the primary targets, in order to evaluate the effects of targets in the secondary data.

Figure 1 contains extracted test statistic plots from [1] at a fixed parametric order that demonstrate the MC lattice-based algorithm performance (labeled PAMF-SN) and the MC covariance least-squares-based algorithm performance (labeled PAMF-LS) for the three test case conditions. In all cases, the reference found that both parametric MC algorithms yielded

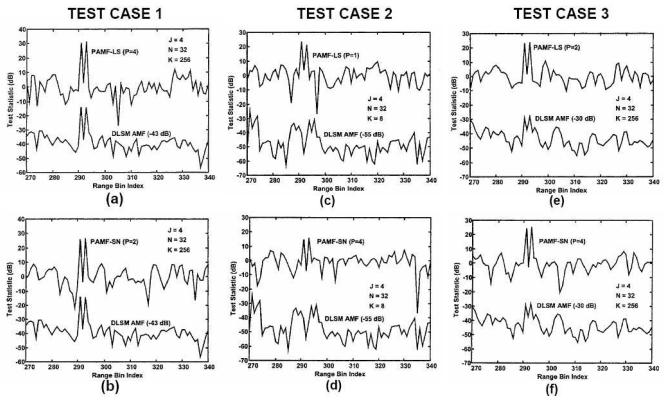

Fig. 1. PAMF-SN and PAMF-LS test statistics from [1] for 3 test cases to compare to 3 new MC and 2D algorithms.

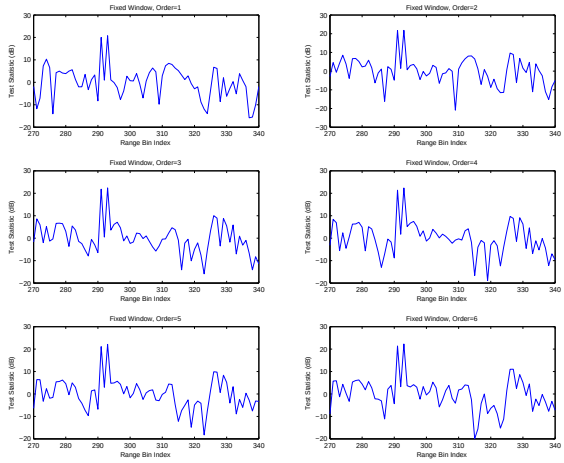

Fig. 2. Test Case 1 (fixed-window filter and two primary targets): PAMF-SN test statistics of multi-channel lattice algorithm for MC orders 1 to 6.

better detection statistics than the conventional non-parametric adaptive matched filter (AMF) algorithm approach. Figures 2-8 are test statistic plots of the two revised MC SN and LS algorithms and the new 2D algorithm over a range of parametric orders from 1 to 6. The reader will notice that the performance is not very sensitive to model order, so comparison will be made with Figure 1 performance at the order indicated in that figure. All plots were normalized to set the mean value to 0 dB for common referencing. Of interest as indicators of the quality of the test statistics are two number pairs: (1) the max target peak above the 0 dB reference level and (2) the difference between the target peak value and the highest non-target peak value (desire large values for both of these numbers). In Figures 2 and 3 at order 3 for test case 1, the new SN and LS MC algorithms produced number pairs of (23dB,13dB) and (22dB,14dB) respectively, compared to (25dB,16dB) and

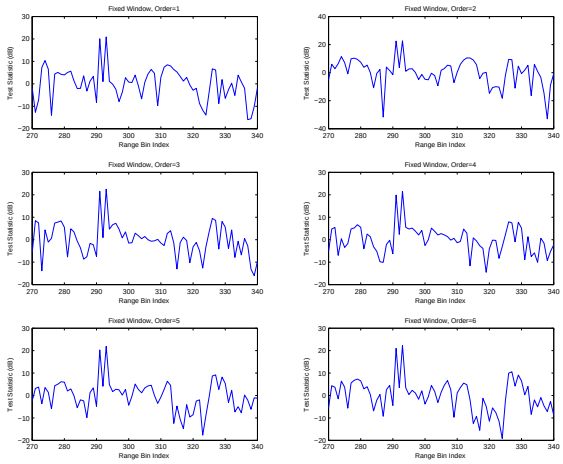

Fig. 3. Test Case 1 (large fixed-window filter and two primary targets): PAMF-LS test statistics of multi-channel covariance least squares algorithm for MC orders 1 to 6.

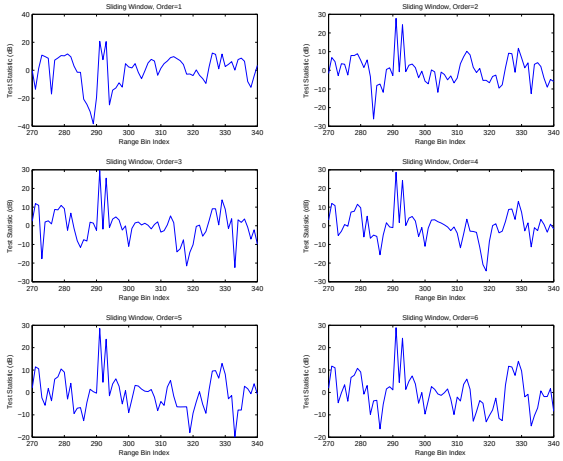

Fig. 4. Test Case 2 (short moving-window filter and two primary targets): PAMF-SN test statistics of multi-channel lattice algorithm for MC orders 1 to 6.

(31dB,19dB) in Figure 1(a)(b). In Figures 4 and 5 at order 3 for test case 2, the improved SN and LS MC algorithms produced number pairs of (32dB,22dB) and (23dB,13dB) respectively, compared to (25dB,16dB) and (22dB,11dB) in Figure 1(c)(d). In Figures 6, 7, and 8 for test case 3, the new SN and LS MC algorithms and the new 2D algorithm produced number pairs of (29dB,17dB), (24dB,13dB), and (22dB,10dB) respectively, compared to (15dB,6dB) and (21dB,11dB) for the MC cases in Figure 1(e)(f).

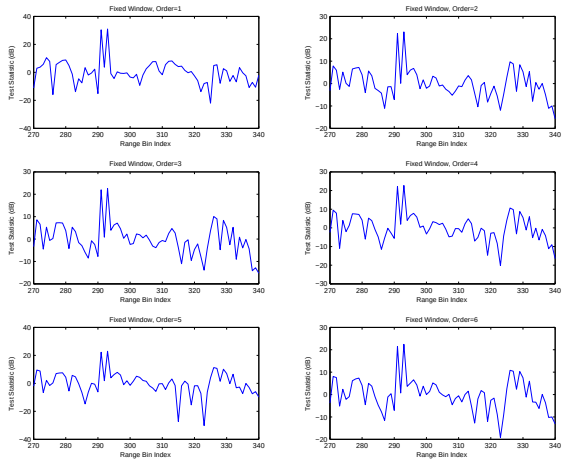

Fig. 5. Test Case 2 (short moving-window filter and two primary targets): PAMF-LS test statistics of multi-channel covariance least squres algorithm for MC orders 1 to 6.

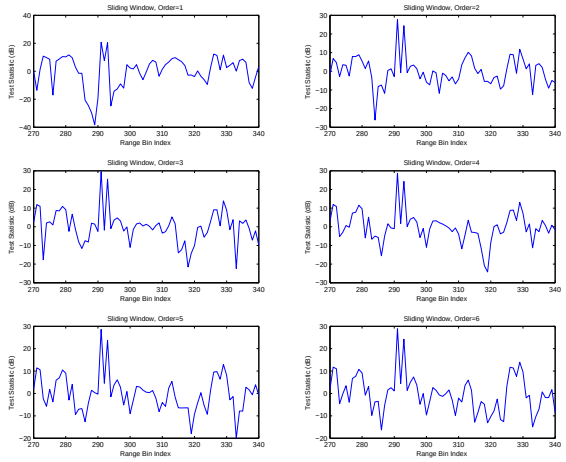

Fig. 6. Test Case 3 (large fixed-window filter, two primary targets, four secondary data targets): PAMF-SN test statistics of multi-channel lattice algorithm for MC orders 1 to 6.

5. REFERENCES

[1] M. Rangaswamy, J. Roman, D. Davis, Q. Zhang, B. Himed, and J. Michels, "Parametric adaptive matched filter for airborne radar applications,", *IEEE Trans. Aerosp. Electron. Syst.*, vol. 36, pp. 677–692, Apr. 2000.

[2] M. Rangaswamy, M. C. Wicks, R. Adve, and T. B. Hale, "Space-time adaptive procesing: a knowledge-based perspective for airborne radar," *IEEE Signal Processing Mag.*, vol. 23, pp. 51–65, Jan. 2006.

[3] S. L. Marple, Jr., *Digital Spectral Analysis with Applications*, Englewood Cliff, NJ: Prentice Hall, 1987.

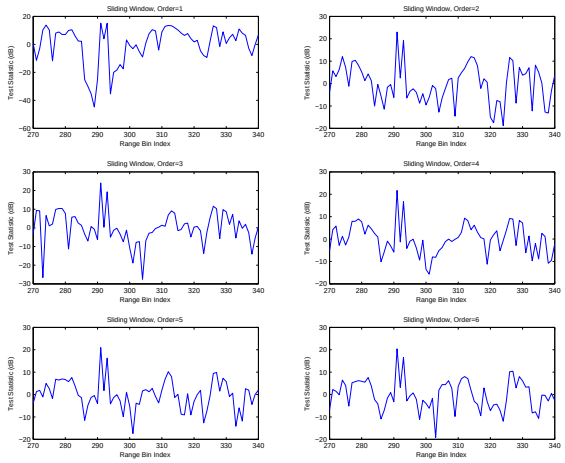

Fig. 7. Test Case 3 (large fixed-window filter, two primary targets, four secondary data targets): PAMF-LS test statistics of multi-channel lattice algorithm for MC orders 1 to 6.

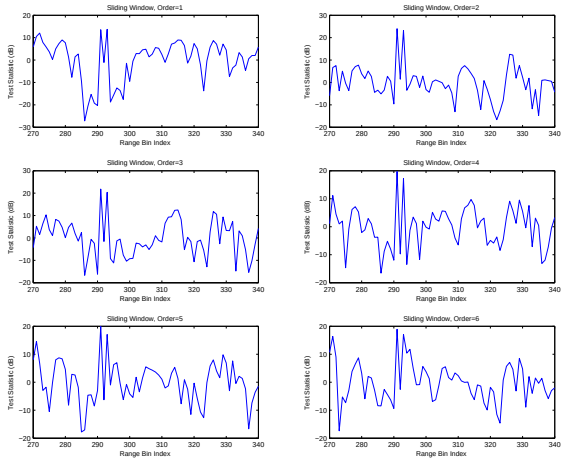

Fig. 8. Test Case 3 (large fixed-window filter, two primary targets, four secondary data targets): PAMF-2D test statistics of two dimensional lattice algorithm for 2D orders 1 to 6 in pulse dimension and fixed order 2 in array channel dimension.

[4] S. L. Marple, Jr., "Two-dimensional lattice linear prediction parameter estimation and fast algorithm," *IEEE Signal Processing Letters*, vol. 7, pp. 164-168, June 2000.

[5] S. Marple, Jr., P. Corbell, and M. Rangaswamy, "New non-stationary target feature detection techniques", presented at 2006 *Asilomar Conf. Signals, Systems, and Computers*.

[6] S. L. Marple, Jr., P. M. Corbell, and M. Rangaswamy,"Multi-channel parametric estimator fast block matrix inverses," presented at 2007 *IEEE Conf. Acous., Speech, Sig. Proc.*.

Very Fast Algorithms and Detection Performance Of Multi-Channel and 2-D Parametric Adaptive Matched Filters for Airborne Radar Applications

Larry Marple

School of EECS
Oregon State University
Corvallis, OR 97331

marple@eecs.oregonstate.edu

Phil Corbell & Murali Rangaswamy

Air Force Research Laboratory
Sensors Directorate
Hanscom AFB, MA 01731

phillip.corbell@hanscom.af.mil
muralidhar.rangaswamy@hanscom.af.mil

Adaptive Sensor Array Processing Workshop

5 June 2007

Dr. Marple's research supported by the AFOSR under the Summer Faculty Fellowship Program.
Dr. Rangaswamy's research supported by AFOSR under Project 2304.

AIRBORNE RADAR SURVEILLANCE APPLICATION

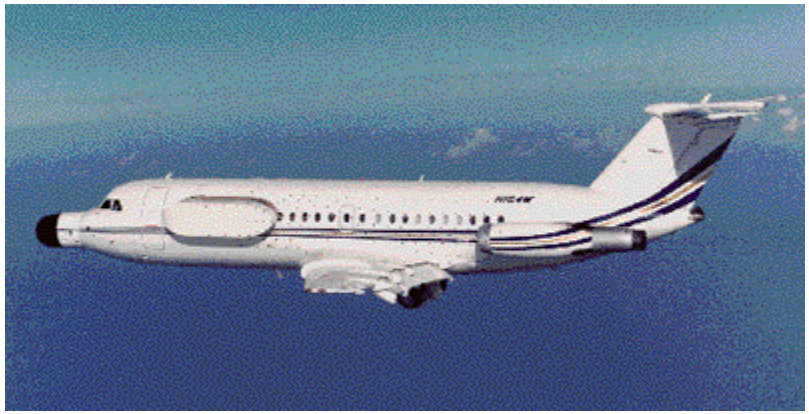

MCARM: Multi-Channel Airborne Radar Measurement Platform

ULA: Uniform Line Array
UPA: Uniform Planar Array

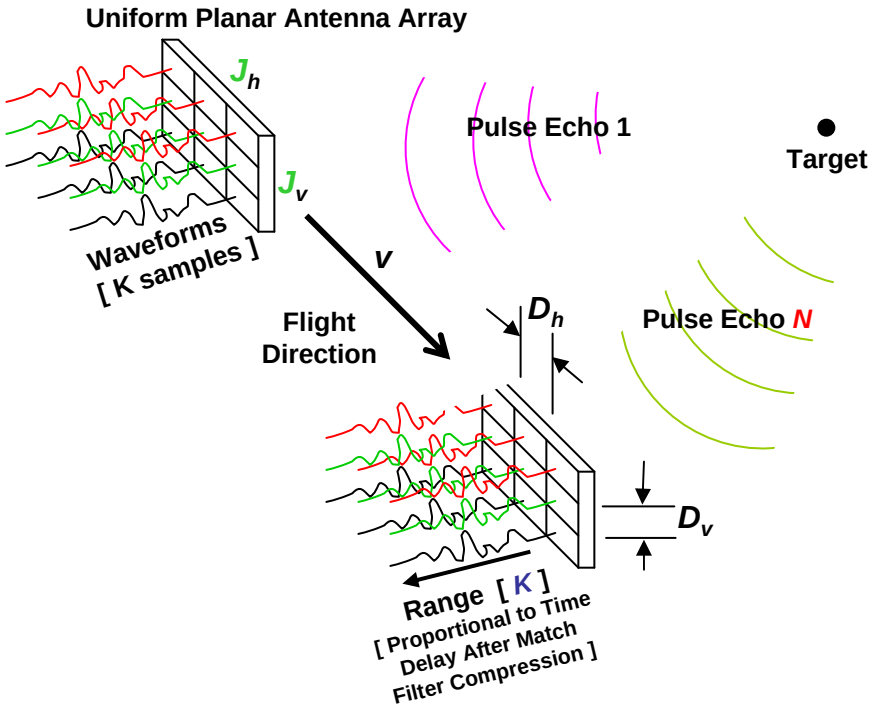

Data is four-dimensional (4-D)

$$J=22 \quad (J_h \times J_v) \times N \times K$$

J_h	J_v	N	K
11	2	128	630
Array Row ULA (AZ Angle)	Array Col. (EL Angle)	Pulses (Slow Time)	Range Bins (RBs) (Fast Time After Pulse Compression)

DATA ORGANIZATION POSSIBILITIES

- **Multi-Channel (M-C) + "Realizations" [window of range bins (RBs)]**

$$x_{jn}[k]$$

Note: Numbers shown are for MCARM radar data.

Conventional multi-channel STAP configuration for arbitrary array geometry or non-uniform phase centers of planar array elements ["channel" is a paired antenna element position and a pulse number]

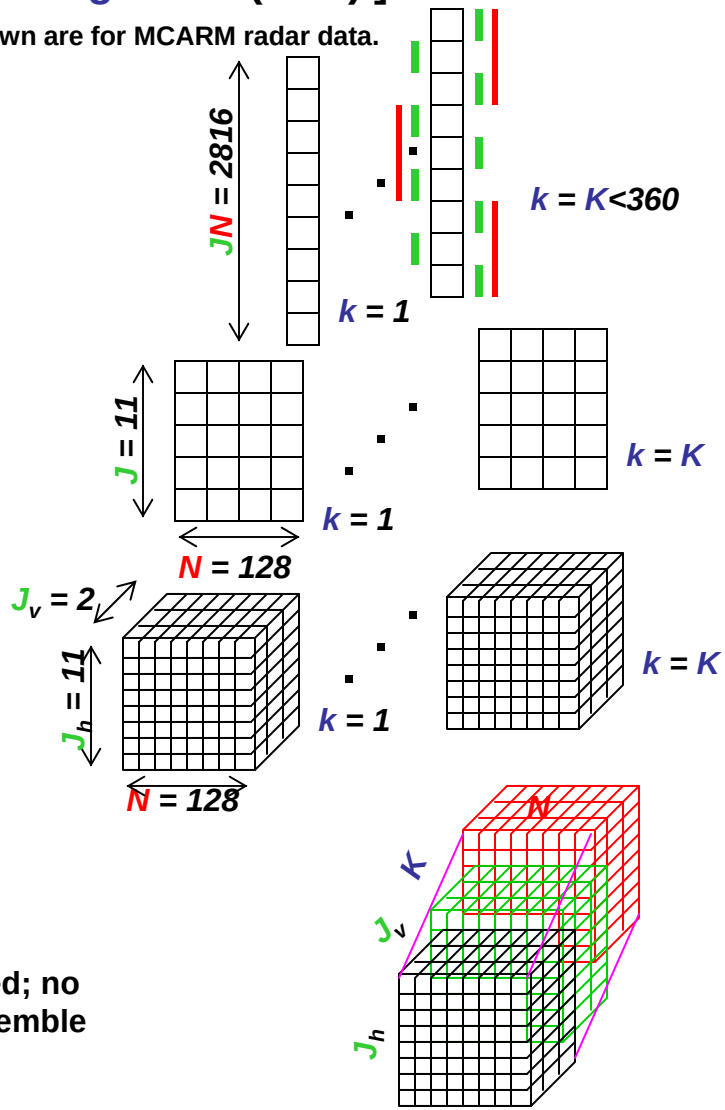

- **Two-Dimensional (2-D) + "Realizations" (RBs)**

$$x[j_h, n; k]$$

Appropriate for uniform line arrays (ULAs) [or a single row of an UPA]

- **Three-Dimensional (3-D) + "Realizations" (RBs)**

$$x[j_h, j_v, n; k]$$

Appropriate for uniform planar arrays (UPAs) [both rows & cols]

- **Four-Dimensional (4-D)**

$$x[j_h, j_v, n, k]$$

All dimensions of data are used; no dimension is available for ensemble "realizations"

MATCHED FILTER AND DETECTION STATISTIC

H means complex conjugate transpose
T means transpose

- **M-C Linear Combiner / Waveformer:** $y = \mathbf{w}^H \mathbf{x}$

  uses *JN* (# antenna array elements x # pulses) M-C data vector:

$$\mathbf{x} = \left[x_{11} \ldots x_{J1} x_{12} \ldots x_{J2} \cdots x_{1N} \ldots x_{JN} \right]^T$$

- **M-C Waveformer MSE Weights To Create Matched Filter** $\mathbf{w}_{MF} = \underline{\mathbf{R}}_d^{-1} \mathbf{e}$

  in which $\underline{\mathbf{R}}_d$ is the *JN* x *JN* M-C target-free "disturbance" covariance matrix and $\mathbf{e}$ is a *JN* x 1 desired steering vector of the receiver array (a function of wavelength, spatial spacings, angles of arrival, PRI, target velocity)

- **M-C Matched Filter Waveformer Output**

$$y_{MF} = \mathbf{w}_{MF}^H \mathbf{x} = \mathbf{e}^H \underline{\mathbf{R}}_d^{-1} \mathbf{x}$$

Usually evaluated for *M* values of e (normalized Doppler freqs. or normalized AOA directions); *M* = 256 to1024 is nominal

- **M-C DETECTION STATISTIC: Normalized Magnitude of Matched Filter Output**

$$\Lambda_{MF} = \frac{\left| \mathbf{e}^H \underline{\mathbf{R}}_d^{-1} \mathbf{x} \right|^2}{\left(\mathbf{e}^H \underline{\mathbf{R}}_d^{-1} \mathbf{e} \right) \left(\mathbf{x}^H \underline{\mathbf{R}}_d^{-1} \mathbf{x} \right)}$$

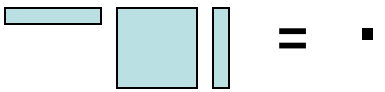

- **DETECTION STATISTIC COMPARED TO A Pr{*fa*} THRESHOLD FOR DETECTION**

ALGORITHM DEVELOPMENT OBJECTIVES

- **COVARIANCE MATRIX INVERSE ESTIMATION STRATEGIES THAT :**
  - **Significantly reduce computational requirements**
    - **Inversion of covariance matrix**
    - **Evaluation of matched filter vector-matrix products**
  - **Reduce secondary (training; RBs) data requirements**
  - **Increase detectability for same or less data**

- **APPROACHES THAT USE :**
  - **Parametric vs non-parametric estimation techniques**
  - **Least square error (LSE) vs mean square error (MSE)**
  - **Primarily multi-channel (M-C) structures; also try 2-D structures**

STRUCTURAL FORMS OF COVARIANCE MATRIX

- Assume uniform PRI (equi-spaced *N*) and ULA ($J=J_h$ and $J_v=1$)
- Multi-channel (M-C) form (uncalibrated array)

$$\underline{R}_d =$$

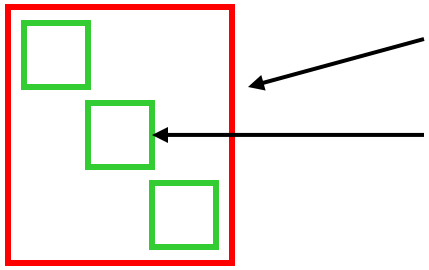

Block *N* x *N* Toeplitz and Hermitian symmetry

Element *J* x *J* dimension without special structure

N blocks

- Two-dimensional (2-D) form (calibrated array)

$$\underline{R}_d =$$

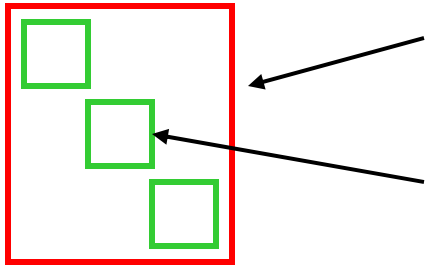

Block *N* x *N* Toeplitz and Hermitian symmetry

Element *J* x *J* Toeplitz without special symmetry

N blocks

CONVENTIONAL NON-PARAMETRIC APPROACH

- **Formulation of non-parametric test statistic**
- **Often referenced as the *Adaptive Matched Filter* (AMF) test statistic**
- **Generate covariance matrix estimate from range-indexed data vectors**

$$\hat{\underline{R}}_d = \frac{1}{K}\sum_{k=1}^{K} x[k]x[k]^H \qquad \text{order } K\left(JN\right)^2$$

- **Compute covariance matrix inversion** $\hat{\underline{R}}_d^{-1}$ **order** $\left(JN\right)^3$

- **Form MF quadratic product terms** $e^H \hat{\underline{R}}_d^{-1} x$, $e^H \hat{\underline{R}}_d^{-1} e$, $x^h \hat{\underline{R}}_d^{-1} x$
  for a range of *M* steering vector *e* values using x data vector not in $\hat{\underline{R}}_d^{-1}$

order $M\left(JN\right)^2$

ALTERNATIVE APPROACH #1 OVERVIEW : MSE-BASED M-C AR PARAMETRIC INVERSE

- **Range-indexed data → M-C autoregressive (AR) block *J* x *J* parameter estimates (several M-C algorithms)**

- **Express inverse in terms of products of block triangular matrices formed from the block AR parameters**

$$\underline{\hat{R}}_d^{-1} = \sum^{1 or 2} \; \cdots \; \mathbf{H} \; \begin{matrix} 0 & \\ & 0 \end{matrix} \; \cdots$$

block diagonal matrix with inverses of error covariances along diagonal

block triangular matrices with block AR parameters

- **Quadratic product terms exploit block triangular matrices to reduce computational evaluation. Example:**

$$e^H \underline{\hat{R}}_d^{-1} x = \underbrace{e^H \; \cdots \; \mathbf{H} \; \begin{matrix} 0 & \\ & 0 \end{matrix} \; \cdots}_{\text{special triangular matrix-vector products}} \; \underbrace{x}_{\text{special triangular matrix-vector products}}$$

ALTERNATIVE APPROACH #2 OVERVIEW : LSE-BASED M-C LP PARAMETRIC INVERSE

- Not forced to use block-Toeplitz form of #1 MSE-based approach
- Inverse $\hat{\underline{R}}_d^{-1}$ replaced by inverse of block-data matrix product $\left(X_d^H X_d \right)^{-1}$

  X_d = rectangular block-Toeplitz structure formed by stacking $x[k]$ data vectors
- Range-indexed data → M-C linear prediction (LP) block ***J*** x ***J*** parameter estimates (two M-C LP algorithms*)
- Express inverse in terms of products of block triangular matrices formed from the block M-C LP parameters

$$\left(X_d^H X_d \right)^{-1} = \sum^{4} \; \cdots \; H \; \begin{matrix} 0 & \\ & 0 \end{matrix} \; \cdots$$

block diagonal matrix with inverses of least squared error sums along diagonal

block triangular matrices with block LP parameters

- Quadratic product terms exploit block triangular matrices to reduce computational evaluation. Example:

$$e^H \left(X_d^H X_d \right)^{-1} x = \underbrace{e^H \; \cdots \; H \; \begin{matrix} 0 & \\ & 0 \end{matrix} \; \cdots}_{\text{special triangular matrix-vector products}} \; \underbrace{\cdots \; x}_{\text{special triangular matrix-vector products}}$$

special triangular matrix-vector products

* Marple: *Digital Spectral Analysis*, Prentice Hall, 1987 (chap.15) and two-volume *Signal Analysis*, 2008

1-D MOTIVATIONAL EXAMPLE : MINIMUM VARIANCE SPECTRAL ESTIMATION

- **Order *p* minimum variance (Capon) spectral estimators**
  - **MSE-based form (Toeplitz covariance matrix)**

$$P_{\text{MV-MSE}}(f) = \frac{1}{e^H(f) R^{-1} e(f)} \quad \text{for} \quad -\frac{1}{2T_s} \le f \le \frac{1}{2T_s} \quad , \quad T_s = \text{sample interval}$$

$$e^H(f) = \begin{bmatrix} 1 & \exp(-j2\pi f T_s) & \cdots & \exp(-j2\pi p T_s) \end{bmatrix} \quad , \quad R = \begin{pmatrix} r[0] & r^*[1] & \cdots & r^*[p] \\ r[1] & r[0] & \ddots & \vdots \\ \vdots & \ddots & \ddots & r^*[1] \\ r[p] & \cdots & r[1] & r[0] \end{pmatrix}$$

  - **LSE-based form (non-Toeplitz covariance-like data matrix product) for data record of *N* samples**

$$P_{\text{MV-LSE}}(f) = \frac{1}{e^H(f)\left(X^H X\right)^{-1} e(f)} \quad , \quad X^T = \begin{pmatrix} x[p+1] & \cdots & x[N-p] & \cdots & x[N] \\ \vdots & \ddots & & \ddots & \vdots \\ x[1] & \cdots & x[p+1] & \cdots & x[N-p] \end{pmatrix}$$

- **Performance test case: 3 complex sinusoids in additive white noise (5 dB SNR)**

1-D MOTIVATIONAL EXAMPLE : PERFORMANCE COMPARISON

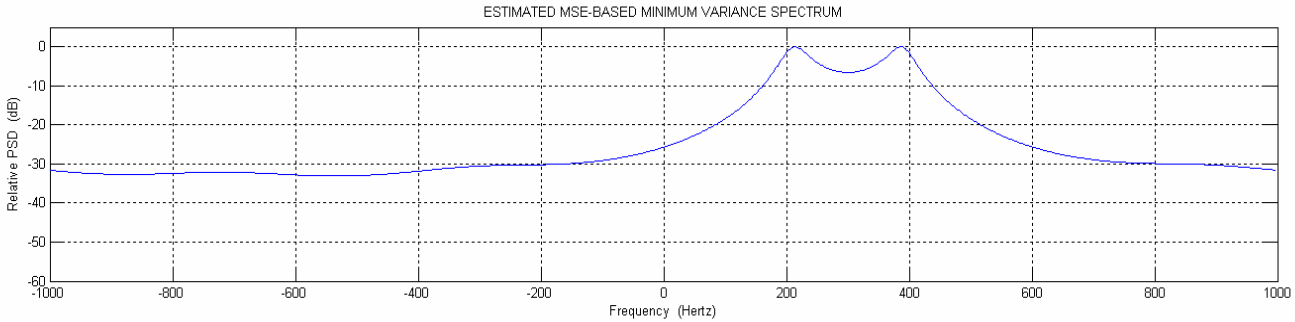

MSE-Based (Data Correlation) Minimum Variance Spectral Estimate

N=200 samples

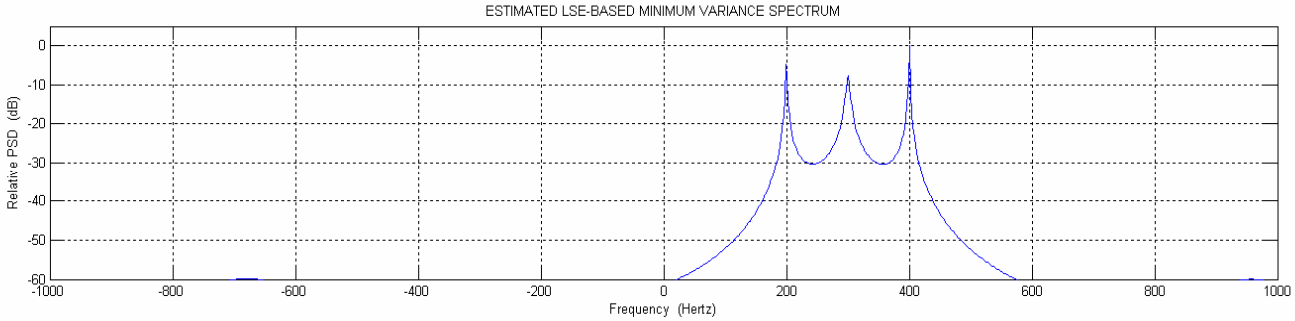

LSE-Based (LP Correlation) Minimum Variance Spectral Estimate

N=200 samples

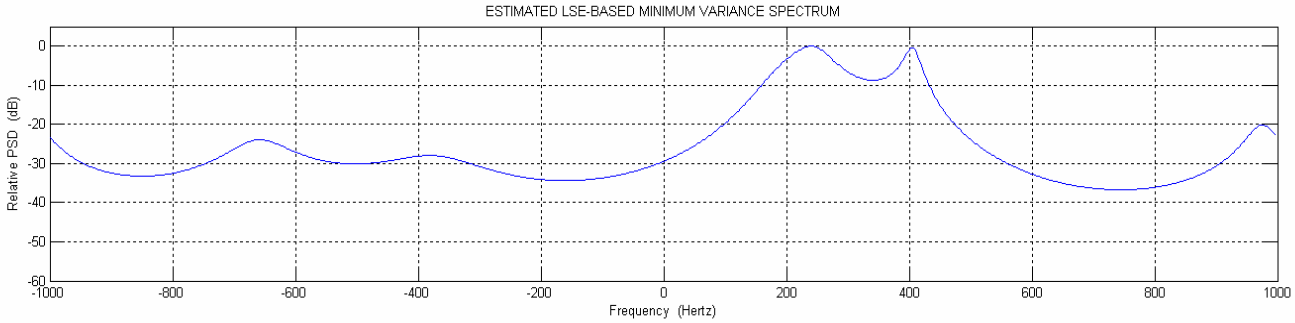

LSE-Based Minimum Variance Spectral Estimate

N=14 samples

All spectral estimates above are order *p* = 6

1-D MOTIVATIONAL EXAMPLE : BASIS FOR MSE-BASED FAST ALGORITHM

- **Covariance matrix R_p is Toeplitz**
- **Non-Toeplitz triangular decomposition (Cholesky)**

$$R_p^{-1} = \begin{pmatrix} \rho_0^{-1} & 0 & 0 \\ 0 & \rho_1^{-1} & 0 \\ 0 & 0 & \rho_2^{-1} \end{pmatrix} \begin{pmatrix} 1 & a_2[1] & a_2[2] \\ 0 & 1 & a_1[1] \\ 0 & 0 & 1 \end{pmatrix}^H \begin{pmatrix} 1 & a_2[1] & a_2[2] \\ 0 & 1 & a_1[1] \\ 0 & 0 & 1 \end{pmatrix}$$

Note that all orders from 1 to *p* are used

- **Toeplitz triangular decomposition (Gohberg-Semencul)**

$$R_p^{-1} = \begin{pmatrix} \rho_2^{-1} & 0 & 0 \\ 0 & \rho_2^{-1} & 0 \\ 0 & 0 & \rho_2^{-1} \end{pmatrix} \begin{pmatrix} 1 & a_2[1] & a_2[2] \\ 0 & 1 & a_2[1] \\ 0 & 0 & 1 \end{pmatrix}^H \begin{pmatrix} 1 & a_2[1] & a_2[2] \\ 0 & 1 & a_2[1] \\ 0 & 0 & 1 \end{pmatrix} + \begin{pmatrix} \rho_2^{-1} & 0 & 0 \\ 0 & \rho_2^{-1} & 0 \\ 0 & 0 & \rho_2^{-1} \end{pmatrix} \begin{pmatrix} 0 & a_2^*[2] & a_2^*[1] \\ 0 & 0 & a_2^*[2] \\ 0 & 0 & 0 \end{pmatrix}^H \begin{pmatrix} 0 & a_2^*[2] & a_2^*[1] \\ 0 & 0 & a_2^*[2] \\ 0 & 0 & 0 \end{pmatrix}$$

Note that only order *p* is used

- **Obtain AR parameters by solution of Yule-Walker equations (Levinson)**

$$\begin{pmatrix} r[0] & r^*[1] & r^*[2] \\ r[1] & r[0] & r^*[1] \\ r[2] & r[1] & r[0] \end{pmatrix} \begin{pmatrix} 1 \\ a_2[1] \\ a_2[2] \end{pmatrix} = \begin{pmatrix} \rho_2 \\ 0 \\ 0 \end{pmatrix}$$

1-D MOTIVATIONAL EXAMPLE : MSE-BASED FAST ALGORITHM

- **Substituting parametric inverse covariance matrix yields**

$$P_{\text{MV-MSE}}(f) = \frac{1}{e^H(f)R_p^{-1}e(f)} = \frac{1}{\sum_{k=-p}^{p}\Psi[k]\exp(-j2\pi fkT_s)}$$

FFT operation !

- **Psi coefficients are autocorrelations of AR parameters (2 FFTs !)**

$$\Psi[k] = \Psi^*[-k] = \begin{cases} \dfrac{1}{\rho_p}\displaystyle\sum_{i=0}^{p-1}(p+1-k-2i)\,a_p[k+i]a_p^*[i] & 0 \le k \le p \\ 0 & k > p \end{cases}$$

- **Many AR parameter estimation algorithms are available :**
  - **Levinson: x → r → a**
  - **Burg: x → a**
- **Fast computational algorithm order:** $Np + 3p\log_2 p$
  Compare to direct covariance matrix inversion: Np^2

1-D MOTIVATIONAL EXAMPLE : LSE-BASED FAST ALGORITHM

- **Fast computational structure of LSE-based MV spectral estimator**

$$P_{\text{MV-LSE}}(f) = \frac{1}{e^H(f)\left(X_p^H X_p\right)^{-1} e(f)} = \frac{1}{\sum_{k=-p}^{p} \Psi[k]\exp(-j2\pi fkT_s)}$$

- **Based on following 4-term triangular Toeplitz inverse structure**

$$\left(X_p^H X_p\right)^{-1} = \text{a} + \text{b} + \text{c} + \text{d}$$

forward LP parameters & lst sqs error sum

backward LP parameters & lst sqs error sum

forward time edge LP gain vector

backward time edge LP gain vector

- **All 4 parameter sets are obtained from the fast solution algorithms* of forward and backward least squares linear prediction**

- **Psi parameter Ψ is the sum of 4 autocorrelations of the 4 parameters (compared to 1 autocorrelation in the prior MSE case, where $b = a^*$)**

- **Overall computational complexity of order $Np^2 + 9p\log_2 p$**

*** Marple: *Digital Spectral Analysis*, Prentice Hall, 1987 (chap.15) and two-volume *Signal Analysis*, 2008**

1-D MOTIVATIONAL EXAMPLE : CONCLUSIONS

- LSE-based minimum variance spectral estimation
  - Fast computational algorithm(s) are available that are competitive with MSE-based versions
  - Better performance is achieved over MSE-based versions (with same data record size)
  - Similar performance is achieved as that of MSE-based versions (with significantly decreased data record size)

BACKGROUND: M-C PARAMETRIC MATCHED FILTER AIRBORNE RADAR APPLICATION

- **Seminal April 2000 IEEE AES Transaction Paper***
  - **Replaced *non-parametric* estimate of covariance inverse with *parametric* est.**
  - **Applied non-Toeplitz triangular inversion formula, so no FFT eval of MF terms**
  - **Used M-C extension of Burg algorithm by Nuttall-Strand** to est. M-C AR terms**
  - **Statistical averaging over range of disturbance-associated data range vectors was applied *outside* M-C AR parameter estimation (post-estimation)**
- **Summer 2006 AFOSR Fellow Study**
  - **Applied Toeplitz triangular inversion formula, so fast FFT eval of MF terms**
  - **Modified M-C Nuttall-Strand algorithm to average range *inside* algorithm**
  - **Applied M-C extension of Marple fast M-C LP algorithm*** to estimate M-C LSE-based LP parameters to use in the inversion formula**
- **Features For Comparison: fast computations and increased performance**

*** Roman, Rangaswamy, Davis, Zhang, Himed, Michels, vol. 36, pp.677-692, 2000**
**** Marple, *Digital Spectral Analysis* (1987) and *** *Signal Analysis* (2008)**

KEY COMPUTATIONAL COMPONENTS OF FAST M-C MSE-BASED PARAMETRIC ALGORITHM

- **Fast M-C MSE-based AR parameter estimation algorithm follows similar approach as 1-D motivational example, except block matrix structure replaces scalar parameters**

$$R_p^{-1} = \begin{pmatrix} (P_2^A)^{-1} & 0 & 0 \\ 0 & (P_2^A)^{-1} & 0 \\ 0 & 0 & (P_2^A)^{-1} \end{pmatrix} \begin{pmatrix} 1 & A_2[1] & A_2[2] \\ 0 & 1 & A_2[1] \\ 0 & 0 & 1 \end{pmatrix} \begin{pmatrix} 0 & 0 & 0 \\ 0 & 0 & 0 \\ 0 & 0 & 0 \end{pmatrix}^H - \begin{pmatrix} (P_2^B)^{-1} & 0 & 0 \\ 0 & (P_2^B)^{-1} & 0 \\ 0 & 0 & (P_2^B)^{-1} \end{pmatrix} \begin{pmatrix} 1 & A_2[1] & A_2[2] \\ 0 & 1 & A_2[1] \\ 0 & 0 & 1 \end{pmatrix} \begin{pmatrix} 0 & 0 & 0 \\ 0 & 0 & 0 \\ 0 & 0 & 0 \end{pmatrix}^H$$

$$\begin{pmatrix} 0 & B_2^*[2] & B_2^*[1] \\ 0 & 0 & B_2^*[2] \\ 0 & 0 & 0 \end{pmatrix}$$

dim $JN \rightarrow Jp$
[eg, N=256, p=6]

block order p^2

- **Use enhanced Nuttall-Strand-Marple M-C AR estimation algorithm to get both forward and backward block AR parameters (conjugate relationship does not hold in M-C)**

- **M-C matched filter (MF) evaluation for detection statistic exploits inverse structure**

$$e^H \hat{\underline{R}}_p^{-1} x = \underbrace{e^H \begin{pmatrix} 0 & 0 & 0 \\ 0 & 0 & 0 \\ 0 & 0 & 0 \end{pmatrix}^H}_{} \underbrace{\begin{pmatrix} 0 & 0 & 0 \\ 0 & 0 & 0 \\ 0 & 0 & 0 \end{pmatrix} x}_{}$$

three block FFTs,
block order $3p \log_2 p$

special block linear convolution products (only 1 of 2 terms shown)

EXPERIMENTAL BASIS FOR PARAMETRIC ORDER

ACTUAL MCARM RADAR DATA

Spectral Power

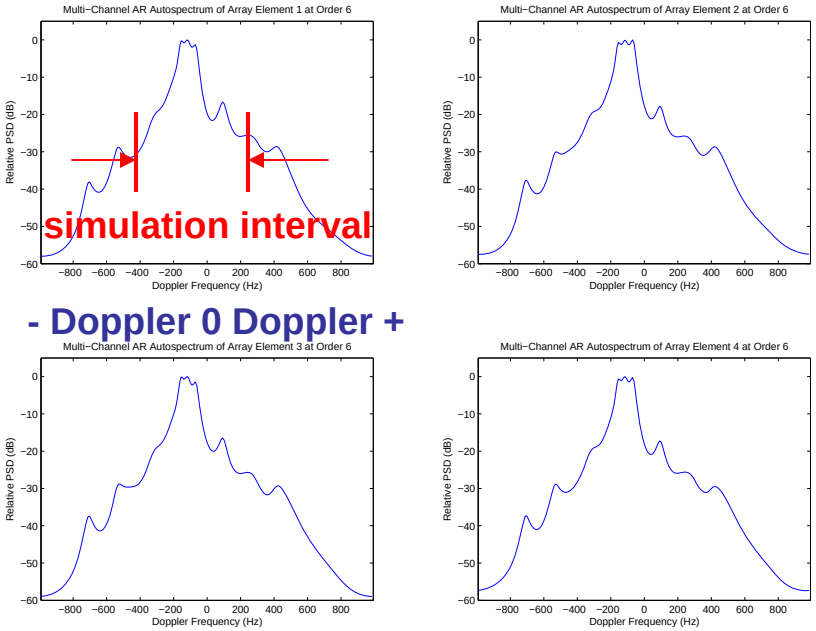

SIMULATED RADAR DATA

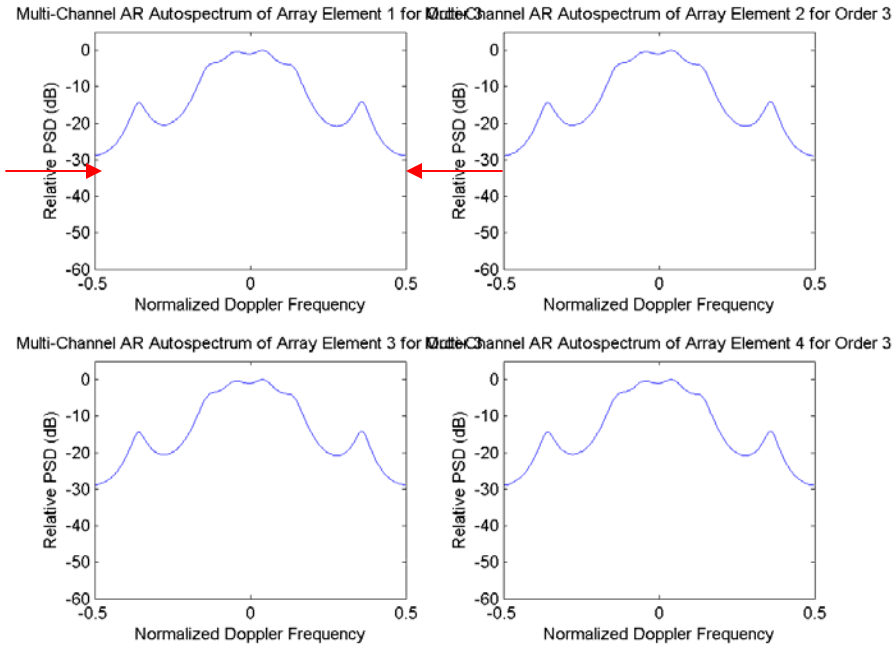

Conditions:

1. **Sensor array channels 1 to 4 shown (out of 22)**
2. **Order 6 MV spectral estimates shown**

KEY COMPUTATIONAL COMPONENTS OF FAST M-C LSE-BASED PARAMETRIC ALGORITHM

- **Similar to M-C MSE-based block parametric algorithm, except have twice as many block triangular components, but can apply block FFT operations**

- **Based on following 4-term block triangular Toeplitz inverse structure***

$$\left(X_p^H X_p\right)^{-1} = \mathbf{a} + \mathbf{b} + \mathbf{c} + \mathbf{d}$$

a: forward block LP parameters & lst sqs error sum

b: backward block LP parameters & lst sqs error sum

c: forward time edge LP block gain vector

d: backward time edge LP block gain vector

dim $JN \rightarrow Jp$
[eg, N=256, p=6]

block order p^2

$$e^H \left(X_p^H X_p\right)^{-1} x = e^H \underbrace{\quad H \quad 0\ 0 \quad}\ \underbrace{\quad}\ x$$

special block linear convolution products (only 1 of 4 terms shown)

* Marple, *Digital Spectral Analysis* (1987) and *Signal Analysis* (2008)

KEY COMPUTATIONAL COMPONENTS OF FAST 2-D MSE-BASED PARAMETRIC ALGORITHM

- **Fast 2-D MSE-based AR parameter estimation algorithm follows similar approach as 1-D motivational example, except block matrix doubly Toeplitz structure replaces scalar Toeplitz parameters**

$$R_p^{-1} = \begin{pmatrix} (P_2)^{-1} & 0 & 0 \\ 0 & (P_2)^{-1} & 0 \\ 0 & 0 & (P_2)^{-1} \end{pmatrix} \begin{pmatrix} 1 & A_2[1] & A_2[2] \\ 0 & 1 & A_2[1] \\ 0 & 0 & 1 \end{pmatrix} \begin{pmatrix} (JP_2^*J)^{-1} & 0 & 0 \\ 0 & (JP_2^*J)^{-1} & 0 \\ 0 & 0 & (JP_2^*J)^{-1} \end{pmatrix} \begin{pmatrix} 0 & JA_2^*[2]J & JA_2^*[1]J \\ 0 & 0 & JA_2^*[2]J \\ 0 & 0 & 0 \end{pmatrix}$$

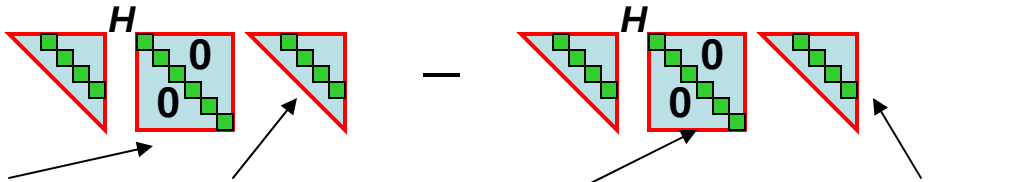

dim $JN \rightarrow p_J p_N$
[eg, J=22, N=256, p_J=4, p_N=6]

block order p_N^2 ,
scalar order $p_J^2 p_N^2$

- **Use 2-D AR estimation algorithm published by Marple [IEEE Signal Processing Letters, 2000] to get 2-D and backward block AR parameters**

- **2-D matched filter (MF) evaluation for detection statistic exploits inverse structure**

$$e^H \hat{R}_p^{-1} x = \underbrace{e^H \begin{pmatrix} H \\ 0 \\ 0 \end{pmatrix}}_{\text{special block doubly Toeplitz linear convolution products (only 1 of 2 terms shown)}} x$$

PERFORMANCE COMPARISONS

- **SIMULATED RADAR ARRAY DATA**
  - **Motivated by MCARM data collection**
  - **Six measurements conditions investigated (3 shown here)**
  - **Plot probability of detection vs output SINR for fixed Pr{*fa*}**
- **ACTUAL RADAR ARRAY DATA (MCARM public data)**
  - **Subset of total available data**
  - **Three test cases with artificially inserted target and interference signals**
  - **Plot MC or 2D detection statistic vs range (about 20 Km)**

SIMULATION PARAMETERS

- Based on Ward's Clutter Model
  - Side-looking GMTI Scenario; modeled after April 2000 IEEE Paper

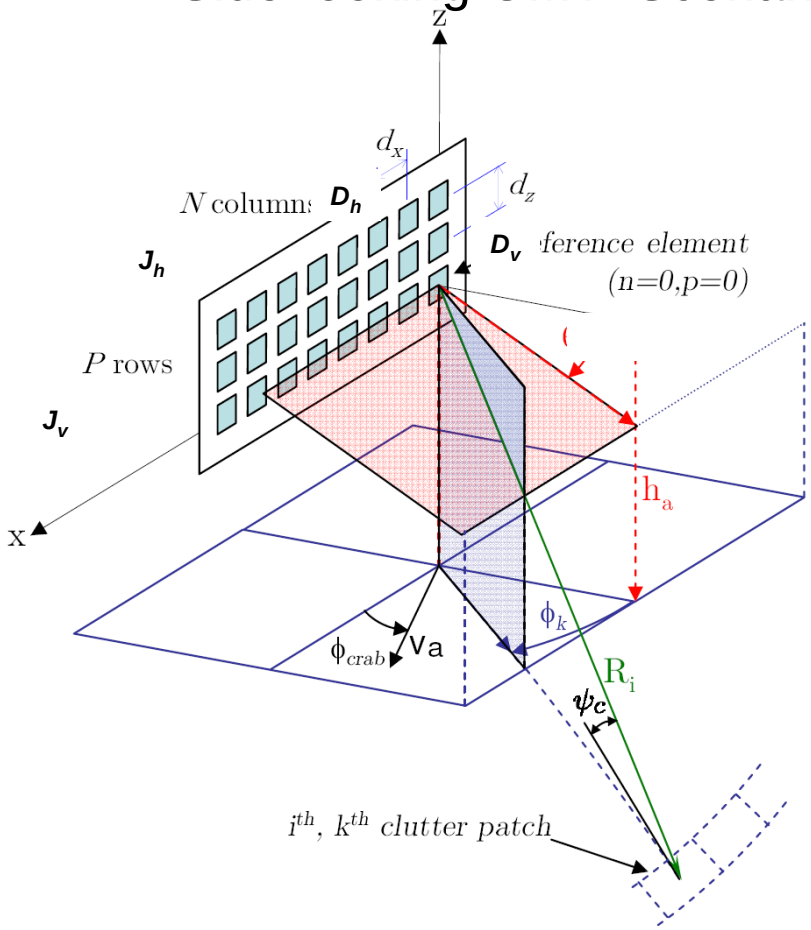

- MCARM-like scenario
- 40 dB Clutter-to-Noise (CNR) Ratio
- 2 Jammers (some cases)
- 20^0 Crab (some cases)
- J=4 Elements
- N=32 Pulses
- Sample support (either):
  - K=256 range bins
  - K=8 range bins

SUMMARY OF SIMULATED TEST CONDITIONS

- **SIMULATED TEST CONDITIONS CONSIDERED**
  1: Large training set, no crabbing, no shared-angle interferers
  2: Small training set, no crabbing, no shared-angle interferers
  3: Large training set, crabbing, no shared-angle interferers
  4: Small training set, crabbing, no shared-angle interferers
  5: Large training set, no crabbing, two interferers
  6: Small training set, no crabbing, two interferers

- **PERFORMANCE MEASURE: dB offset to right of ideal MF clairvoyant response (shown on next slide) at P_d of 0.5 (represents roughly the performance degradation of the curve)**

- **PERFORMANCE SUMMARY TABLE**

	M-C Lst Sqs Lattice		M-C Geometr. Lattice		M-C Lst Sqs Linear Predict.		2-D Lst Sqs Lattice	
	2006 Study	2000 Study	2006 Study	2000 Study	2006 Study	2000 Study	2006 Study	2000 Study
Test Case 1	-0.5 dB	-1 dB	-0.5 dB	--	-0.5 dB	-0.5 dB	-0.5 dB	--
Test Case 2	-7.5 dB	-8 dB	-0.7 dB	--	-0.5 dB	-0.5 dB	-1.2 dB	--
Test Case 3	-0.8 dB	-1 dB	-1.0 dB	--	-0.8 dB	-0.8 dB	-3.0 dB	--
Test Case 4	-3.5 dB	-3.5 dB	-1.0 dB	--	-0.8 dB	-0.8 dB	-3.0 dB	--
Test Case 5	-0.6 dB	-0.6 dB	-0.6 dB	--	-0.6 dB	-0.6 dB	-1.2 dB	--
Test Case 6	-2.5 dB	-2.5 dB	-1.2 dB	--	-0.6 dB	-0.6 dB	-1.5 dB	--

- **LstSqs LP (MC-LLS) performs most robustly with little variations across all test conditions**
- **Few tenths dB improvement of improved LstSqs Lattice algorithm (MC-CLS 2006) over MC-CLS 2000 algorithm version for several test conditions**

SIMULATED TEST CONDITION #1

J=4 Array Elements, N=32 Pulses, K=256 Fixed Range Bin Window
No Crab Angle, No Interferers Added, Order p=3

2006 Study

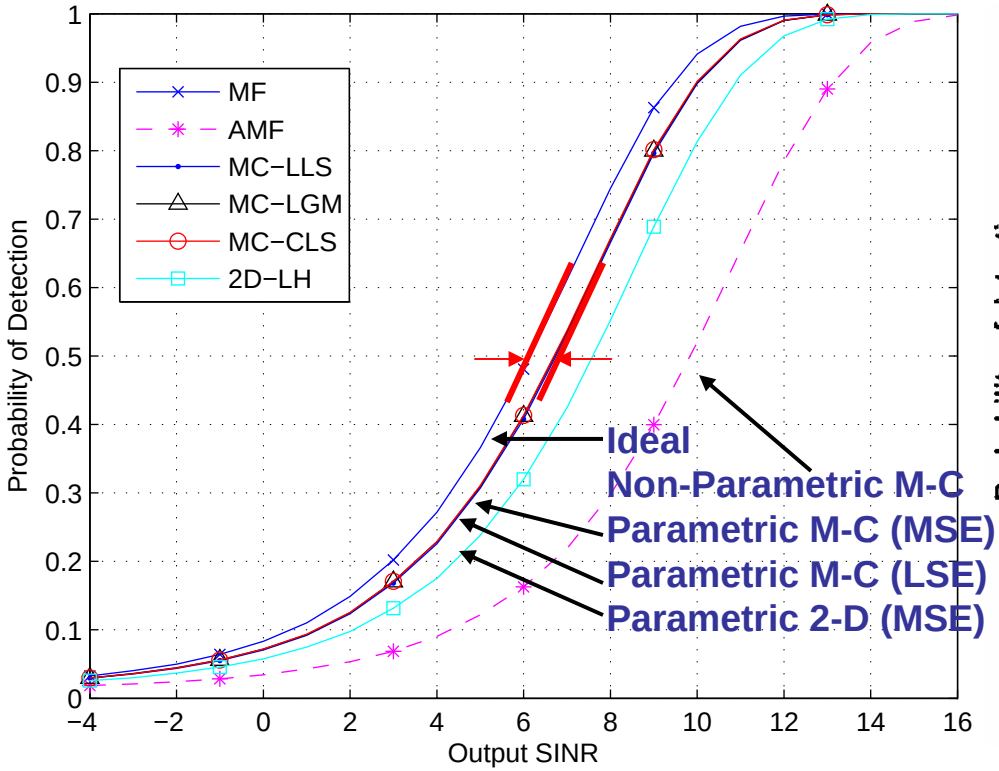

2000 Study

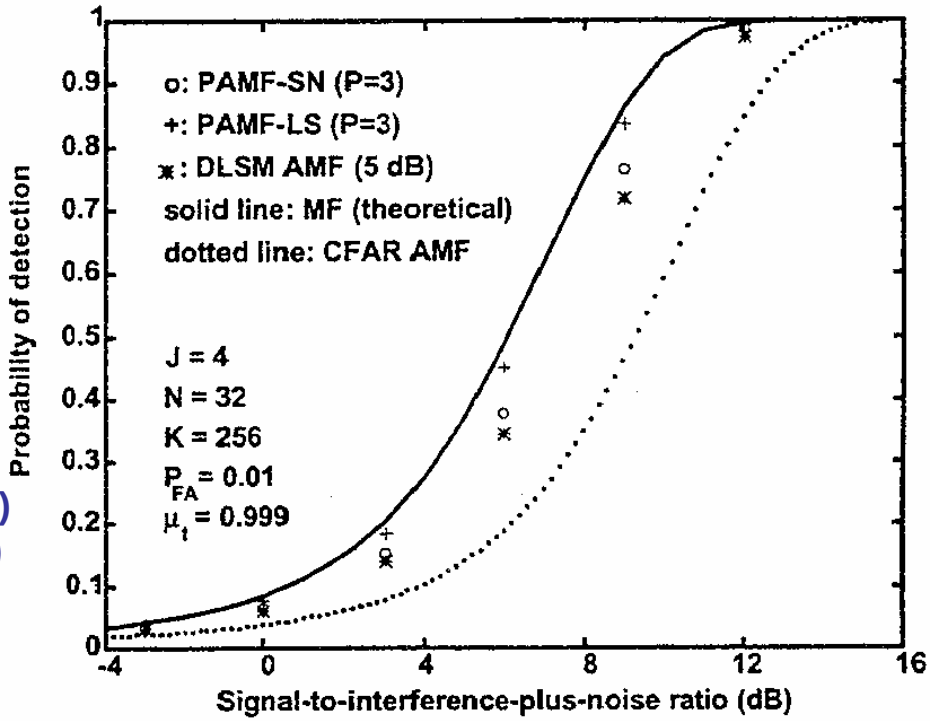

SIMULATED TEST CONDITION #2

J=4 Array Elements, N=32 Pulses, K=8 Moving Range Bin Window
No Crab Angle, No Interferers Added, Order p=3

2006 Study

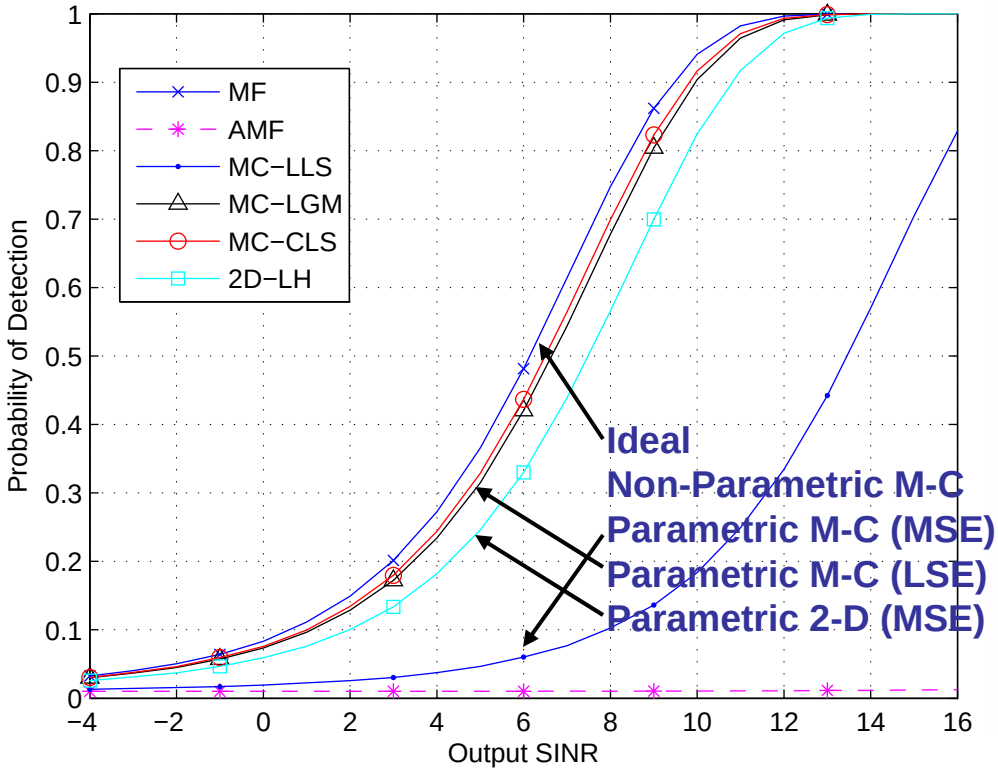

2000 Study

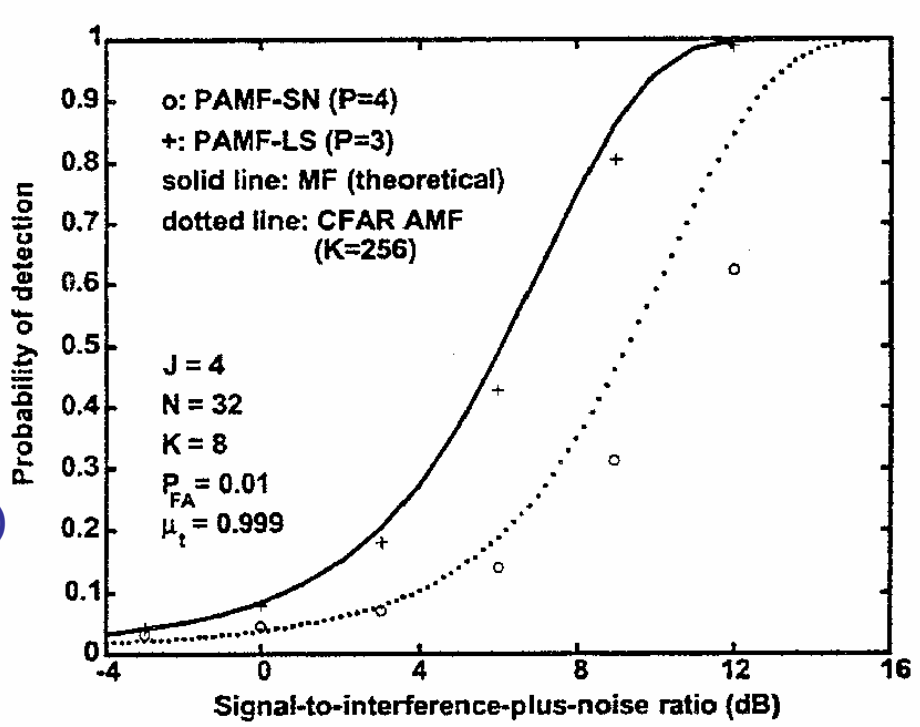

SIMULATED TEST CONDITION #6

J=4 Array Elements, N=32 Pulses, K=8 Moving Range Bin Window
No Crab Angle, 2 Jammers Added, Order p=3

2006 Study

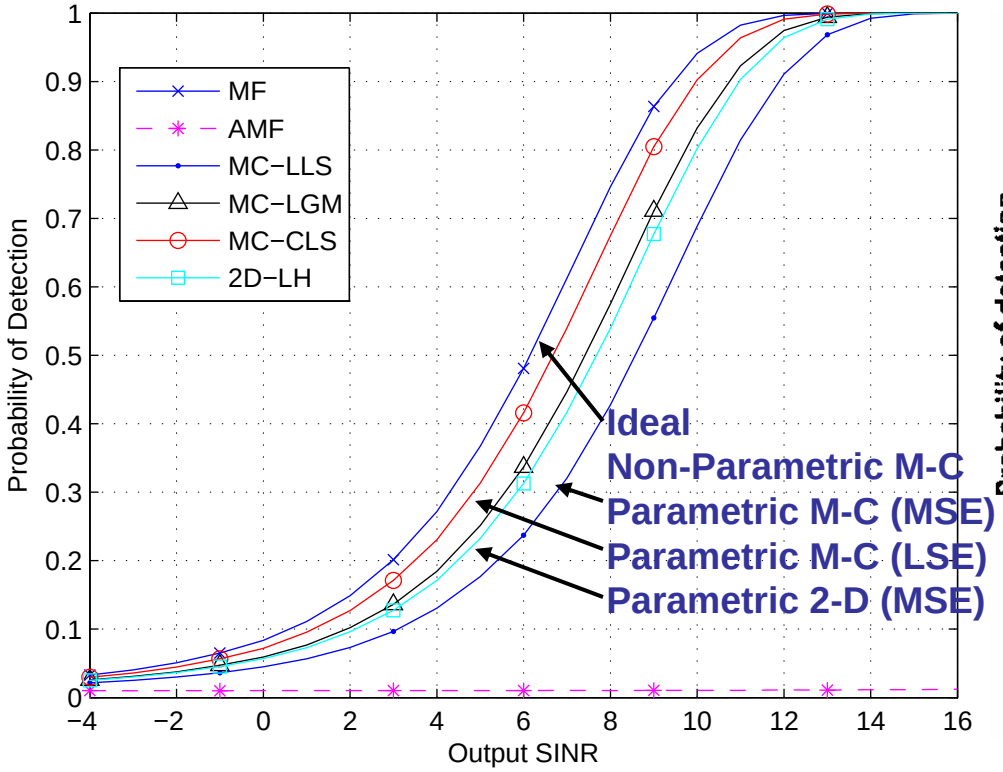

2000 Study

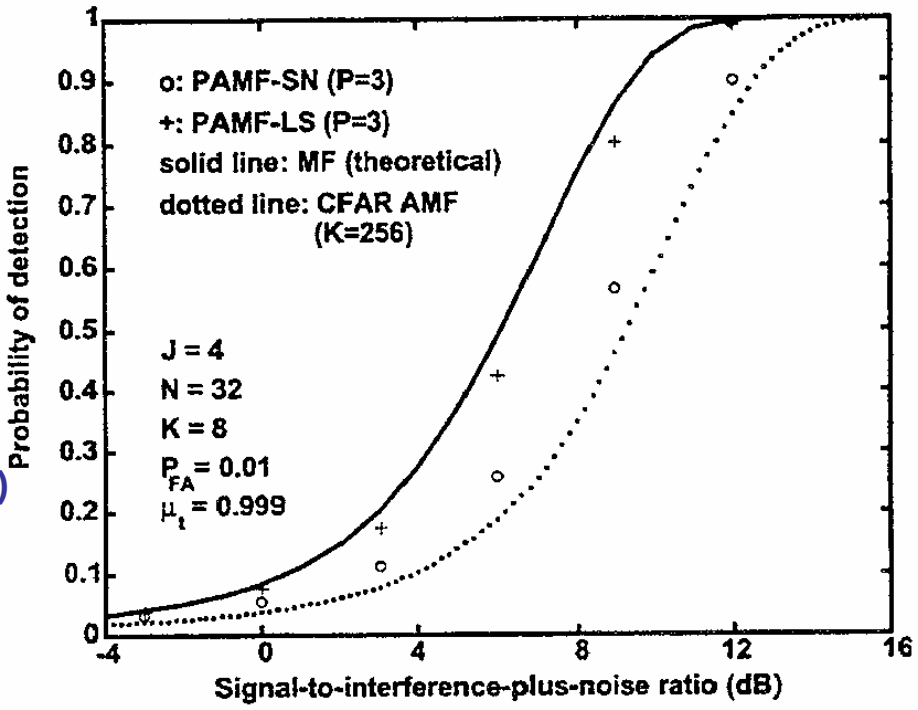

CONCLUSIONS

- **Parametric covariance matrix fast inversion algorithms for :**
  - **Enhanced M-C MSE-based (force block Toeplitz) inversion developed**
  - **M-C LSE-based (non-block-Toeplitz) inversion introduced**
  - **2-D MSE-based (force doubly Toeplitz) inversion developed**

- **Using the non-parametric inversion approach as the baseline, the relative computational requirements and performance as averaged over the 3 simulations shown were :**
  - **M-C MSE-based algorithm was .7 x baseline in computations and -.5 dB from exact MF, vs -2.8 dB for non-parametric baseline**
  - **M-C LSE-based algorithm was 1.1 x baseline in computations and -.5 dB from exact MF, vs -2.8 dB for non-parametric baseline**
  - **2-D MSE-based algorithm was .2 x baseline in computations and -.5 dB better than baseline**

BACKUP #1 :
ACTUAL MCARM RADAR TEST CONDITIONS

- Performance using actual MCARM radar data with injected artificial target signals.
- Test statistic magnitude vs range bin index for acquisition 575, flight 5 for 1 el ch, 4 az channels, 32 pulses, RBs 142-469 inclusive.
- Test cases:
  - Case 1: fixed windows 256 RBs (142-269,341-468), injected SINR -30dB at RB 291 and 293; plot RBs 270-340.
  - Case 2: moving window 11 RBs (8 used); otherwise same conditions as Case 1
  - Case 3: 4 secondary interfering targets of same doppler added in RBs 238, 269,373, 400 at -10 dB input SINR
- Performances not sensitive to model order.
- Measures: max target peak above the 0dB reference level; difference between target peak value and highest non-target peak value (want both to be large)
- Prior paper found AMF poor relative to PAMF.
- All plots normalized to common mean level of 0 dB to set reference level
- LEFT FIGURE: 2006 Study ; RIGHT FIGURE: 2000 Study

BACKUP #2 : ACTUAL DATA TEST CASE 3-- MSE-BASED M-C AR PARAMETRIC ALGORITHM

J=4 Array Elements, N=32 Pulses, K=256 Fixed Range Bin Window, 4 Interferers

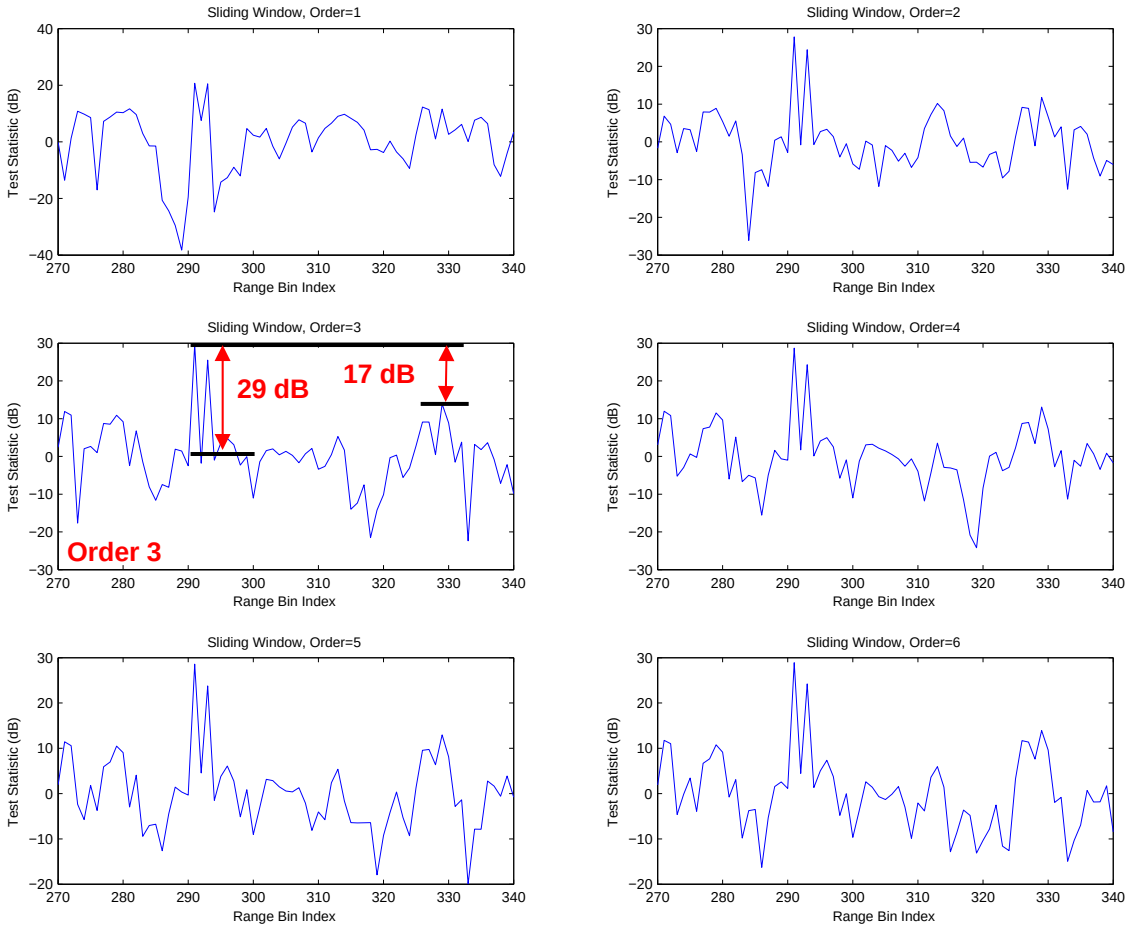

2006 STUDY (orders 1 to 6)

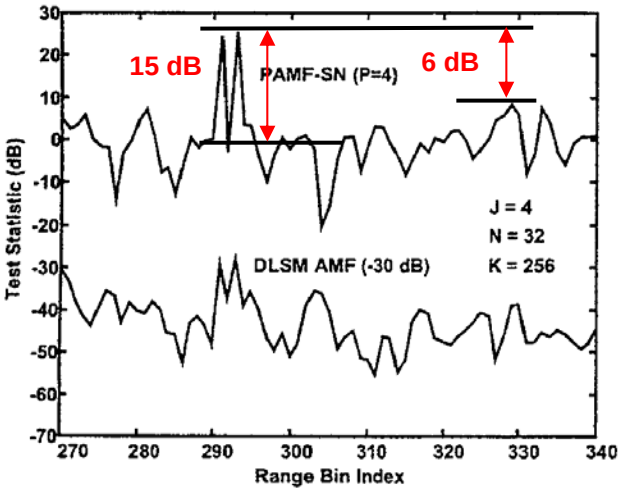

2000 STUDY (order 4)

BACKUP #3 : ACTUAL DATA TEST CASE 3-- LSE-BASED M-C LP PARAMETRIC ALGORITHM

J=4 Array Elements, N=32 Pulses, K=256 Fixed Range Bin Window, 4 Interferers

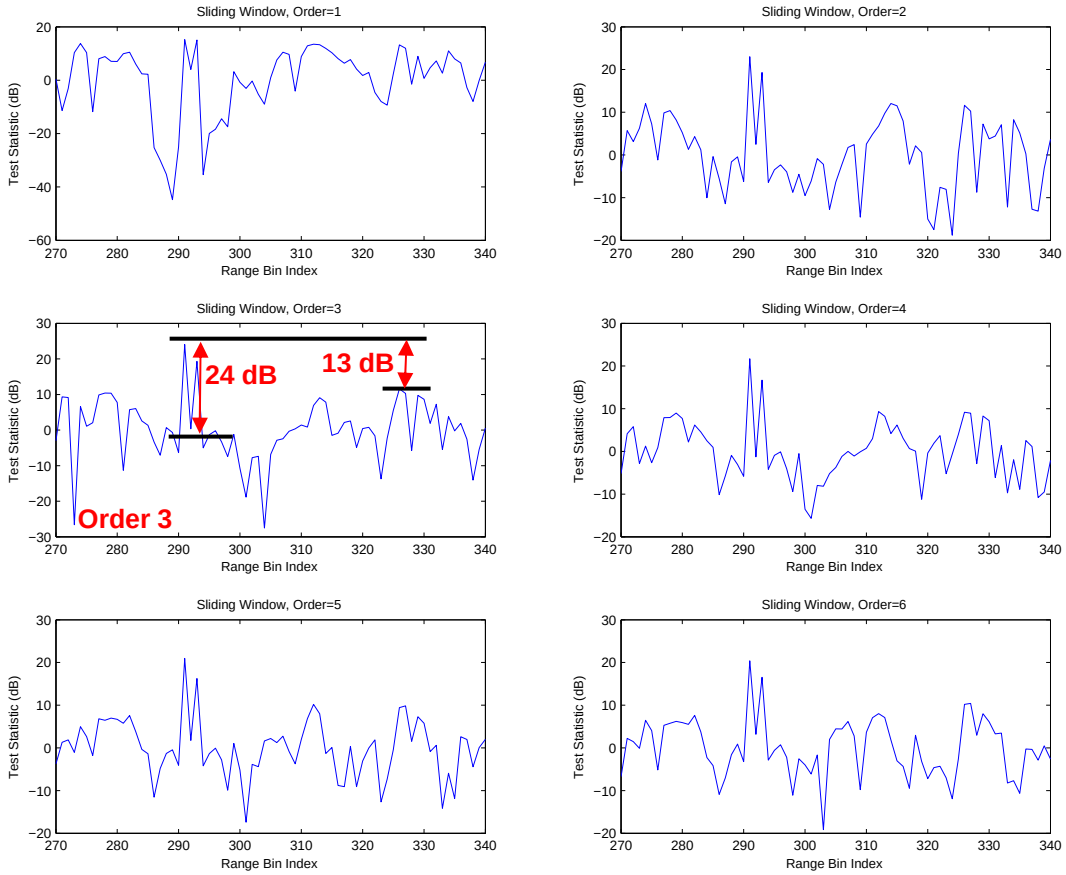

2006 STUDY (orders 1 to 6)

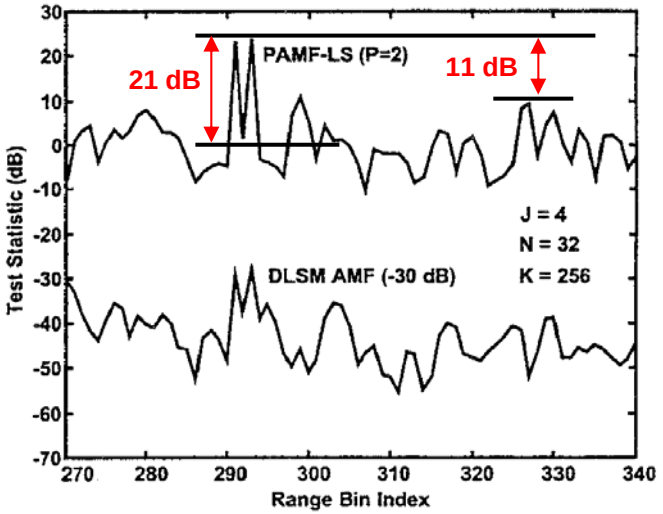

2000 STUDY (order 2)